Int. J. Heat Mass Transfer. Vol. 27, No. 1, pp. 125–136, 1984
Printed in Great Britain

0017–9310/84 $3.00 + 0.00

A NEW ANALYSIS OF THE CLOSED LOOP THERMOSYPHON

JOHN E. HART
Department of Astrogeophysics, University of Colorado, Boulder, CO 80309, U.S.A.

(*Received* 6 *January* 1983 *and in revised form* 25 *May* 1983)

Abstract—This theoretical study addresses the nature of motions in a toroidal fluid loop oriented in the vertical plane and subject to rather general internal heating and/or thermal wall conditions. It is shown that previous one-dimensional models of flow in the loop can be transformed, without further approximation, to a 'master' problem of three non-linear ordinary differential equations, along with an infinite set of linear 'slaved' problems. The mass flux is determined solely by the master problem. The question of existence and stability of steady flows reduces to a study of cubic algebraic equations. In the strongly non-linear regime, it is argued that only steady or chaotic flows, not periodic ones, are possible. The sensitivity of the one-dimensional model predictions to various wall-stress parameterizations is described.

NOMENCLATURE

- A amplitude of oscillatory disturbances on the steady flow
- B factor in the stability equation (19b)
- C_d drag coefficient
- C_n nth cosine mode amplitude
- Δc supercriticality, equation (21)
- f drag law function, equation (17)
- g gravitational acceleration
- h heat transfer coefficient
- h' non-dimensional heat transfer function, equation (9)
- n Fourier expansion index
- N drag law exponent, equation (17)
- Pr flow parameter, equation (8a) (effective Prandtl number)
- q mass flux
- q_s applied surface heat flux
- Q internal heating rate
- R_0 radius of torus
- R_p cross-sectional radius of torus
- Ra' flow parameter (effective Rayleigh number)
- Ra_c critical Rayleigh number
- S_n nth sine mode amplitude
- t time
- T temperature
- T^* effective driving temperature distribution, equation (4)
- T_d non-dimensional driving temperature distribution
- T_w external wall temperature
- ΔT internal temperature scale
- ΔT_e effective driving temperature scale for T^* of equation (4)
- v azimuthal cross-sectionally averaged velocity
- V velocity scale.

Greek symbols

- α angle of symmetry axis of torus with respect to horizontal
- β coefficient of thermal expansion
- λ Landau constant
- ρ basic fluid density
- τ wall stress
- θ azimuthal angle around torus with respect to torus axis.

1. INTRODUCTION

THERE has recently been much interest in convectively driven flows in closed or open fluid loops. The flow in a rectangular closed pipe heated at the bottom branch and cooled along the top branch was originally studied by Welander [1] as a crude but informative model for naturally occurring convection in unconfined regions. Subsequently Torrance [2] and Bau and Torrance [3] have proposed various pipe models for geophysical flows in the earth's crust. In the past few years much of the experimental and theoretical work on convective flows in closed tubes has been oriented toward applications in solar heating systems, where the loop is usually heated at locations below the points of cooling so that the mass and heat transfer around the loop is self-driven (e.g. no pumps are needed). Such systems are called thermosyphons. Recent research has sought an understanding of the dynamics of flows in such heated circuits, especially whether or not the motion is steady, oscillatory, or even chaotic, and of how the internal fluxes are related to the external parameters.

The prototypical example of the thermosyphon is shown in Fig. 1. It is basically a torus oriented in the vertical plane, containing a working fluid of constant viscosity and thermal diffusivity. The radii of the tube and torus are R_p and R_0, respectively. The fluid is driven by a distribution of temperature around the walls, $T_w(\theta)$, or perhaps by an internal heat source $Q(\theta)$ [J m^{-3} s^{-1}], where θ is the angle around the torus starting from an offset angle α that measures the rotation of the symmetry axis of the torus up from the horizontal. The significance of the offset angle is discussed further below. The internal heat source $Q(\theta)$ in practice can be generated by radiative fluxes, Joule heating, or more commonly by a thermal flux condition at the inside of the torus wall. In this last instance $Q(\theta)$ is just the flux at

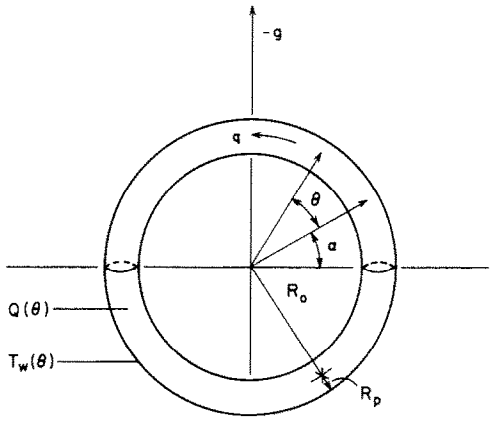

FIG. 1. Geometry and heating conditions for the thermally driven fluid loop.

the wall, $q_s(\theta)$ say, divided by $R_p/2$. Other specific heating methods have been considered in the literature but it will be seen that they are mathematically equivalent to those shown in Fig. 1.

Of principal interest here is the time dependence of the mass flux q, and the distribution of temperature around the torus for various heating distributions. Previous research on this system has concentrated on the study of one-dimensional (1-D) models for the flow. That is, cross-sectional averages are taken perpendicular to the circumferential axis of the torus. The non-linear terms in the momentum and energy equations are replaced by interactions between the averaged temperature and the averaged azimuthal mass flux only. This is equivalent to neglecting the averaged Reynolds stress in the usual mean and turbulent flow decomposition. Although recent two-dimensional (2-D) numerical work by Mertol *et al.* [4] indicates significant departures from 1-D behavior, if the averaging is done carefully (with appropriate factors for the non-linear interactions), 1-D models provide a useful and qualitatively accurate description of the observed motions, and they have received much attention. Creveling *et al.* [5] studied the case with $\alpha = 0$, a constant wall flux inwards for negative θ (the lower half of the torus), and constant T_w for positive θ. They found that steady flow solutions of the 1-D model equations agreed with experiment only if the wall-stress parameterization in terms of the mass flux varied with the applied heating rate. For low heating rates, frictional drag was proportional to q, while at higher values the actual internal motion appeared to be turbulent and the stress seemed to follow a $q^{1.5}$-law. Using these friction laws they computed the stability of the predicted steady flows by deriving a transcendental characteristic equation for the linear growth rates that had an infinite number of roots. The stability results gave partial agreement with experiment. Greif *et al.* [6] integrated the 1-D thermosyphon model with linear drag using a finite-difference representation in θ to obtain further information about the predicted transient behavior of the simple loop. These two studies have been extended to other situations of practical importance. Mertol *et al.* [7] discuss steady 1-D solutions and stability in the presence of throughflow. Damerell and Schoenhals [8] study the predicted and observed steady flow, as well as the observed flow instability in a system where the symmetry axis of the heating and cooling is slanted with respect to gravity ($\alpha \neq 0$). As α goes from 0 to 90°, the physical situation goes from bottom-heated to side-heated. As α is increased from zero there are substantial changes in the flow which are of importance for the solar thermosyphon problem.

In this paper a new approach to the study of the 1-D thermosyphon model is presented. First it is shown that the set of non-linear partial differential equations (in θ and t) used in the previous studies can be reduced to three coupled non-linear ordinary differential equations. This major simplification makes it a very simple task to investigate the existence of steady solutions and their stability, transient behavior, and strongly non-linear effects like persistence, hysteresis, and chaos. The analysis shows that the general structure of the predicted 1-D flows are remarkably insensitive to the heating distribution, provided it meets some rather weak symmetry restrictions. However, the results appear to be very sensitive to the friction parameterization. For realistic external heating rates typical of previous laboratory work, there appear to be only two types of flow at large times after initial transients have decayed. The motion is either steady, with possible multiple solutions for the same external driving, or chaotic.

2. FORMULATION

Consider the flow in the loop of Fig. 1. Since previous authors [2–8] have derived the 1-D model of the thermosyphon in some detail one can start with the usual azimuthal circulation and thermal energy equations obtained by averaging over the cross-section of the torus and evaluating the wall stress and heat flux empirically. Let $v(t)$ be the average azimuthal velocity at all θ, and $T(\theta, t)$ be the average temperature. Then the circulation and energy equations can be put into the following form [6]

$$\rho \frac{dv}{dt} = \frac{g\rho\beta}{2\pi} \int_{-\pi}^{\pi} T \cos(\theta + \alpha)\, d\theta - \frac{2\tau}{R_p}, \tag{1}$$

$$\rho C_p \frac{dT}{dt} = \rho C_p \left(\frac{\partial T}{\partial t} + \frac{v}{R_0} \frac{\partial T}{\partial \theta} \right) = \frac{-2h(\theta)(T - T_w)}{R_p} + Q(\theta). \tag{2}$$

In these equations ρ is the basic density of the Boussinesq working fluid, C_p the heat capacity, β the coefficient of thermal expansion, g the gravitational acceleration, τ the wall stress, t the time, and h the heat transfer coefficient from the wall to the fluid. To close the system τ and h must be specified as functions of

either position, time, and/or the dependent variables of the problem v and T. One supposes that the heat transfer coefficient can be written as

$$h = h_0[1 + h'(\theta)]. \tag{3}$$

That is, the heat transfer has a constant component h_0 as well as a variation with position around the torus. This positional variation can represent changes in wall properties with θ. $T_w(\theta)$ is considered to be an applied temperature on the outside of the toroidal wall. If the wall were thin and of uniform conductivity (in θ), then $h'(\theta)$ would be zero. As a counter-example, Creveling *et al.* [5] have an approximate heat-flux boundary condition for negative θ (using a heater tape wrapped around a glass section of the torus) and a constant temperature boundary condition for positive θ (using an isothermal water jacket surrounding a copper tube). In the present model these external conditions would be emulated by setting $h' = -1$ and $Q = 2q_s/R_p$ for $\theta < 0$, with $Q = h' = 0$ and T_w equal to the water jacket temperature for $\theta > 0$. The convention used throughout is that the range of θ is $-\pi \leqslant \theta \leqslant \pi$.

Equations (1) and (2) are normalized by using a velocity scale V and a time scale R_0/V. It is assumed that the wall stress τ can be written in the general form $\tau = C_d v|v| f(|v/V|)/2$ where $f(|v/V|)$ is a non-dimensional power law function, and C_d is the drag coefficient whose magnitude may depend on the form of f. The temperature is scaled with the dimensional value $\Delta T = 2V^2 C_d/g\beta R_p$. This is the temperature difference between upward and downward sections of the torus required to give a steady flow V that balances the buoyancy torque with a quadratic wall drag.

In addition a combined heating function can be defined as

$$T^*(\theta) = T_w(\theta)[1 + h'(\theta)] + Q(\theta)R_p/2h_0. \tag{4}$$

In this model internal heating (or thermal wall fluxes) and temperature conditions at the walls combine into one thermal source term. This effective wall temperature T^* is normalized by a scaling temperature ΔT_e such that the non-dimensional driving temperature $T_d(\theta) = T^*(\theta)/\Delta T_e$ has a peak value of 1.

A velocity scale is used such that

$$V = 2h_0 R_0/\rho R_p C_p. \tag{5}$$

This is the velocity that yields a unit Péclet number in the following sense. It can be considered as the circumferential velocity required to give one circuit around the loop in the time it takes a thermal signal to relax by diffusion by a factor $e^{-2\pi}$ or about 1%. The normalized equations (with v, T, and t henceforth being non-dimensional) then become

$$\frac{dv}{dt} = Pr\left[-f(|v|)|v|v + \frac{\cos(\alpha)}{\pi}\int_{-\pi}^{\pi} T\cos(\theta)\,d\theta - \frac{\sin(\alpha)}{\pi}\int_{-\pi}^{\pi} T\sin(\theta)\,d\theta\right], \tag{6}$$

$$\frac{\partial T}{\partial t} + v\frac{\partial T}{\partial \theta} = -T(1 + h') + Ra'\,T_d(\theta). \tag{7}$$

The two non-dimensional parameters are

$$Pr = R_0 C_d/R_p, \tag{8a}$$

and

$$Ra' = \frac{\Delta T_e}{\Delta T} = \frac{g\beta\Delta T_e R_p^3}{8(h_0/\rho C_p)^2 R_0^2 C_d}, \tag{8b}$$

where Pr is an effective inverse Reynolds number. If Pr is large, inertia in the loop is negligible ($dv/dt \approx 0$). This is equivalent to a large Prandtl number in laminar flow with molecular friction. Using equation (5), $Pr = C_d V/V_T$, where $V_T \equiv 2h_0/\rho C_p$ is proportional to the thermal diffusion velocity normal to the walls. Since $C_d V$ is the effective friction velocity, Pr is seen to be a generalized Prandtl number. Similarly, Ra' can be considered as a ratio of the square of the forced buoyancy velocity $g\beta\Delta T_e R_0$ to the product of the circumferential friction velocity $R_0 C_d V/R_p$ and the circumferential thermal diffusion velocity $V_T R_0/R_p$. Thus Ra' is a modified Rayleigh number.

To make further progress it is necessary to place some rather weak but crucial restrictions on $T_d(\theta)$ and $h'(\theta)$. It is required that T_d be an odd function of θ. That is, the driving must be antisymmetric about the line $\theta = 0$. This implies that the θ-average of T^* is zero, or that the thermal fluctuations in the torus are unbiased. Any bias in the heating would simply change the average temperature of the loop. In addition T_d must be symmetric on either side of $\theta = \pi/2$ and $-\pi/2$ in both θ half-planes. In other words the peaks of T_d must be at $\theta = \mp\pi/2$ and T_d must be distributed equally for θ less than or greater than the peak points. These restrictions are not as severe as it might seem. By changing α one can rotate the peaks of the heating with respect to the vertical, and rather general shapes of T_d are allowed provided they are not skewed. All previously reported experiments on tori that the author is aware of satisfy these restrictions.

The present model also requires that the heat transfer coefficient $h'(\theta)$ be constrained to the following form

$$h'(\theta) = 0 \quad \text{for} \quad 0 < \theta < \pi, \tag{9a}$$

$$h'(\theta) = h'(\text{const.}) \quad \text{for} \quad -\pi < \theta < 0. \tag{9b}$$

If $h' \neq 0$ then the model describes a torus with different heat transfer coefficients above and below $\theta = 0$. For example the lower half of the loop might have a higher conductivity ($h' > 0$) compared with the upper half. A special case is $h' = -1$ whence the lower half is an insulator. It could be coated with a thin metallic layer carrying an electrical current. Joule heating in the film would yield a wall flux q_s but with negligible heat loss. In practice such flux conditions are only approximated very crudely [5]. However, it is clear that many other combinations and forms are possible.

The problem then is to solve the non-linear partial differential equations (6) and (7) with a prescribed

driving temperature T_d and h' as given by equations (9a) and (9b). The key to the solution of the problem is to note that the only effect of temperature on the azimuthal velocity v is through the weighted θ integrals of equation (6). The weighting functions $\cos(\theta)$ and $\sin(\theta)$ suggest a solution in discrete Fourier modes. Thus one can expand

$$T(\theta) = \sum_n C_n(t) \cos(n\theta) + S_n(t) \sin(n\theta), \quad (10a)$$

and

$$T_d(\theta) = \sum_n [-H_n \sin(n\theta)], \quad (10b)$$

with

$$H_n = \int T_d \sin(n\theta)\, d\theta/\pi, \quad (10c)$$

where the index n is over all odd integers 1, 3, 5, ..., etc. because of the symmetry conditions outlined above. In summary, if equations (9a) and (9b) are satisfied and equations (10b) and (10c) provide a complete expansion of T_d then the model is exact.

The above expansions are substituted into equations (6) and (7). After multiplying by $\cos(n'\theta)$ and $\sin(n'\theta)$ and integrating over θ, an infinite set of ordinary differential equations for $v(t)$, $S_n(t)$ and $C_n(t)$ are obtained. To put these in a standard form one rewrites $v = X(t)$, $C_1 = Y(t)$, $S_1 = Z(t) - Ra$, and use a slightly redefined velocity scale $V \to (1+h')V$. The new set of transformed equations is then

$$\frac{dX}{dt} = Pr[-X|X|f(X) + \cos(\alpha)Y - \sin(\alpha)(Z - Ra)], \quad (11)$$

$$\frac{dY}{dt} = -XZ - Y + Ra\, X, \quad (12)$$

$$\frac{dZ}{dt} = XY - Z, \quad (13)$$

where $Ra = Ra'\, H_1/(1+h'/2)^2$.

There is also an infinite sequence of quasi-linear problems for the higher θ modes with $n = 3, 5, 7, \ldots$, etc. These are

$$\frac{dC_n}{dt} = -C_n - nXS_n, \quad (14)$$

and

$$\frac{dS_n}{dt} = -S_n + nXC_n + Ra\, H_n/H_1. \quad (15)$$

It can be shown that the structure of the flow in the loop, $X(t)$, is completely determined by the three nonlinear ordinary differential equations (11)–(13) alone. This is because the temperature only contributes to the net torque on the fluid in the torus if it has a component proportional to $\sin(\theta)$ or $\cos(\theta)$. Thus to solve for the motion one only has to solve this 'master' problem involving the $n = 1$ thermal modes.

Looking at equations (14) and (15), it can be argued that given $X(t)$ from the master problem, there will be a unique, convergent, and stable solution of this set of problems provided H_n decays with n. It is shown in the appendix that if X is steady or periodic, the S_n and C_n modes from equations (14) and (15) will be steady or periodic, respectively. Further, numerical integrations not described here show that if X is aperiodic (chaotic) the solutions of these equations will be chaotic as well. Thus the solution of the original 1-D partial differential equations can be reduced to a three-component master problem along with a large set of linear slaved-mode problems the solution of which has no effect on the mass flow. In what follows only the master problem is addressed, since only the nature of the time dependence in the loop, not the detailed thermal distribution for a specific driving term T_d is of interest. Clearly, once $X(t)$ is determined it is a trivial job to find the solutions of the slaved problem for steady flows, and only slightly harder for periodic ones. It is shown below that this latter task is not required since no periodic solutions are found for parameter ranges of practical interest.

3. ANALYSIS OF THE MASTER PROBLEM

The master problem shows firstly that if $H_1 = 0$, so that there is no $\sin(\theta)$ dependence in the heating distribution, $Ra = 0$ and any initial motion in the loop will decay away. Conversely, it is only the $\sin(\theta)$ component of the generalized forcing T^* that affects the dynamics! Thus one considers $H_1 \neq 0$ and proceeds to look at the types of motion allowed.

The problem posed in equations (11)–(13) turns out to contain as a special case one of the most studied mathematical problems in recent years. If $\alpha = 0$ and $f = |v|^{-1}$ these equations are identical to the set of equations originally proposed by Lorenz [9] as a highly truncated model of thermal convection between plane parallel plates. Because the Lorenz equations have chaotic solutions they have been subject to much investigation concerned with the bifurcation sequences that lead in and out of the chaotic regimes (see Ott [10] or Lanford [11] for reviews that contain many of the references to this work). In Lorenz's model Pr was the fluid Prandtl number and Ra the Rayleigh number, although here the parameters have the slightly different interpretations given in Section 2. The Lorenz limit, corresponding to heating antisymmetric about the vertical, and a laminar friction law, is a useful starting point and some of the previous results are reviewed below.

Steady solutions are easily found. They are $X_0 = 0$ and $X_0 = \pm\sqrt{(Ra-1)}$. Thus if $Ra < 1$ the only steady solution is $X_0 = 0$. The two others, corresponding to clockwise and counterclockwise rotation, exist when $Ra > 1$. Lorenz shows that for $Ra > 1$ the null solution is unstable, whereas the two non-zero solutions are stable for Ra less than a critical number

$$Ra_T = Pr(Pr+4)/(Pr-2), \quad (16)$$

which has a minimum value of 14.92 at $Pr = 5.465$. At this critical value of Ra, the linear stability analysis of small perturbations about the steady mode indicates that they should break down via an exponentially growing, oscillatory disturbance. One thus expects a similar sort of behavior for the equations for non-zero α and other friction functions f.

One can now proceed to an analysis of equations (11)–(13) for general α and a friction function

$$f(X) = X^{-N}. \tag{17}$$

Steady solutions are obtained by eliminating Y and Z in favor of X with the time derivatives set to zero. They are given by the equation

$$X_0^{(4-N)} + X_0[X_0^{(1-N)} - \cos(\alpha)Ra] - \sin(\alpha)Ra = 0. \tag{18}$$

When $N = 1$ and $\alpha = 0$ this just gives a quadratic equation for X_0 along with the $X_0 = 0$ solution. When $N = 0$ (quadratic friction) and $\alpha = 0$ there is one real root of the resulting cubic equation along with the null solution. If $N = 1$ (the laminar friction case) and $\alpha \neq 0$ one again obtains a cubic equation but this one can have three real and unequal roots for a fixed set of external parameters. There is thus the possibility of multiple solutions and hysteresis. This is true for the general case of $N \neq 1$ and $\alpha \neq 0$ as well. The existence of multiple real roots at fixed N, Ra, α, and Pr means that various initial states may migrate towards different steady fixed-points. Which fixed-point is selected will depend on how close the initial condition is to, or whether or not it is in the attractor basin of, a given fixed-point. To gain some understanding of which solutions may be allowed it is necessary to consider their stability.

The stability of the steady solutions determined from equation (18) is easily investigated by perturbing equations (11)–(13) about the steady roots. Note that once X_0 is found, equations (12) and (13) give $Y_0 = Ra\, X_0/(1+X_0^2)$, and $Z_0 = X_0 Y_0$. Then assuming perturbations of the form $(x, y, z)\exp(\omega t)$ and linearizing equations (11)–(13), one obtains a simple cubic equation for $\omega(Ra, Pr, \alpha)$

$$\omega^3 + \omega^2[B+2] + \omega[2B+1+Pr\cos(\alpha)(Z_0 - Ra) + X_0^2] + [B(1+X_0^2) + Pr\cos(\alpha)((Z_0 - Ra) + X_0 Y_0) + Pr\sin(\alpha)(Y_0 - X_0(Z_0 - Ra))] = 0, \tag{19a}$$

with

$$B = (2-N)Pr|X_0|^{(1-N)}. \tag{19b}$$

If all the roots have $\mathrm{Re}(\omega) < 0$ then the corresponding steady solution will be stable.

The effect of varying N on the stability of the steady solutions is looked at first. In what follows N is restricted to the usual laminar-turbulent range of parameterizations, e.g. $0 < N < 1$.

Consider the $\alpha = 0$ case first. The steady flows are given by

$$X_0^{(3-N)} + X_0^{(1-N)} = Ra. \tag{20}$$

Temporarily redefining $Ra = Ra\, X_0^n$ leads to a cubic with $\partial Ra/\partial X_0 > 0$. Thus it is seen that this cubic will have only one real root for all Ra. Since the original friction law has the absolute value in it, this root actually gives two solutions of equal magnitude and opposite rotation. This is expected from the physical symmetry; there is a degeneracy between clockwise and counter-clockwise motion when $\alpha = 0$. Without loss of generality one only considers the positive root. The cubic stability equation for ω can be solved by assuming that two of the roots are complex conjugates. That is, assume the full cubic has the factored form $(\omega - i\,\omega_0)(\omega + i\,\omega_0)(\omega - \omega_1)$, where ω_0 is real. Thus one is looking for the neutral curve dividing growing and decaying oscillatory disturbances. Without going into the straightforward algebra, this assumption allows the direct determination of the critical values of $Pr = Pr_c$ as the solution of a quadratic equation whose coefficients are known functions of X_0. This is obviously a much easier method than that used by Creveling *et al.* [5]. Figure 2 gives the lowest values of Pr and Ra for which the steady solution becomes linearly unstable as functions of N. It is seen that the critical $Ra = Ra_c$ increases rapidly as the friction law approaches the turbulent limit $\tau \approx v|v|$ (i.e. $N = 0$). Figure 3 shows the critical values of Pr vs Ra for several values of N. The 'wedges' of instability are largest for the laminar case, decreasing monotonically in size, as N increases. Figure 4 shows the dependence of the neutral frequencies on Ra for the Pr values obtained from Fig. 3. The frequency increases with Ra and is relatively insensitive to Pr. Thus when $\alpha = 0$ one expects on the basis of linear theory to see a transition from the steady solution to an oscillatory one as Ra is increased (e.g. as the heating rates are raised).

When $\alpha \neq 0$ the situation becomes a bit more complicated. Only the steady solutions and their stability for $N = 1$ have been found in detail, although the analysis could easily be carried through for other N. The steady

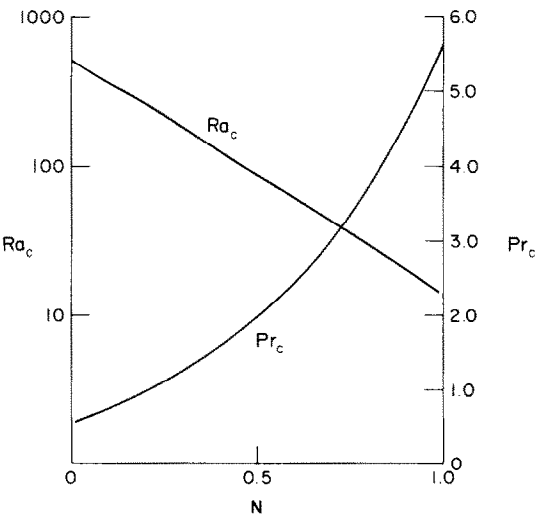

FIG. 2. Critical values of Ra and Pr dividing stable and steady flow from unstable steady flow as a function of the drag exponent N.

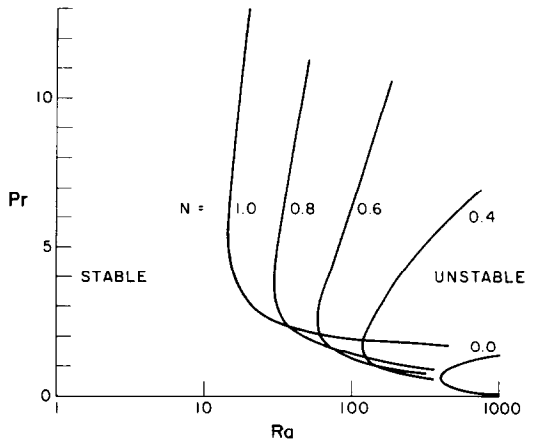

FIG. 3. Neutral curves in the Ra, Pr plane for values of N shown.

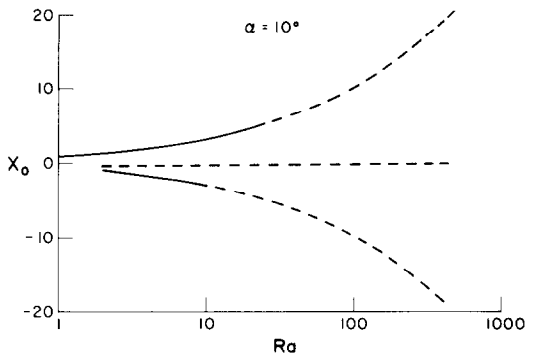

FIG. 5. Steady flow solutions at $Pr = 7.0, \alpha = 10°$. Dashed and solid lines show where steady solutions exist, but only the solid line solutions are stable.

roots are given by

$$X_0^3 + X_0[1 - \cos(\alpha)Ra] - \sin(\alpha)Ra = 0. \quad (21)$$

At low Ra there will only be one real root corresponding to the direct forcing of a circulation by the heating. This heating is not symmetric about the bottom of the loop but is biased on one side and the circulation is up on this side. As Ra is increased a threshold is crossed after which there are three real roots. This occurs when $(1-\cos(\alpha)Ra)^3/27 + \sin^2(\alpha)Ra^2/4 = 0$. One solution is the continuation of the original single root. The others represent two steady flows of rotation in the negative α direction. These solutions are substituted each in turn into equation (19) and their stability analysed.

Figure 5 shows the allowable (e.g. real) steady solutions for X_0 along with their stability for $Pr = 7$. The small and negative root that is bracketed by the larger roots is always unstable to a monotonically growing disturbance. The extreme roots eventually become unstable to an oscillatory mode where the solid curves become dashed. Notice that there is a region of multiple stable solutions where there are two solid lines for the same Ra. These are reflections of the situation at $\alpha = 0$ where two roots exist and are stable, except here, they are not simply equal and opposite since there is side-biased heating present when $\alpha <> 0$. Figures 6 and 7 show the existence and stability results when $\alpha = 30°$ and 60°, respectively. The multiple steady flow region disappears at larger α and the range of Ra over which the co-rotating flow (in the $+\alpha$ direction) is stable increases with α. Thus for low angles of rotation of the heating distribution one might expect to find multiple steady modes with associated hysteresis. At large α there will be only one stable steady solution that ultimately breaks down via an oscillatory perturbation. One might then in this case expect to see oscillatory flows when Ra is made greater than this transition point.

Very similar behavior at other values of Pr was found. For $Pr = 1$ the region of double stable roots extended over a substantially larger range of α and Ra where for $Pr = 20$ the range was considerably smaller than that for $Pr = 7$. Also, just as lowering N increased the region of stability for $\alpha = 0$, it raises substantially the value of Ra necessary to destabilize all three roots when $\alpha <> 0$. For example, at $Pr = 7, \alpha = 30°$, and $N = 0.55$ (approximately the turbulent friction law found experimentally in ref. [5]) the co-rotating steady flow remains stable at least up to $Ra = 1500$.

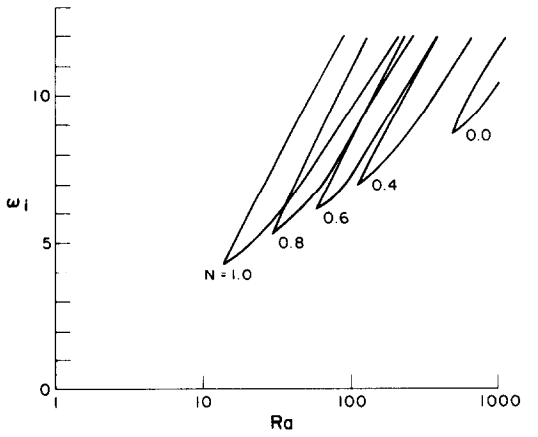

FIG. 4. Frequency of the unstable mode for various N. Upper branches correspond to the upper branches in Fig. 3.

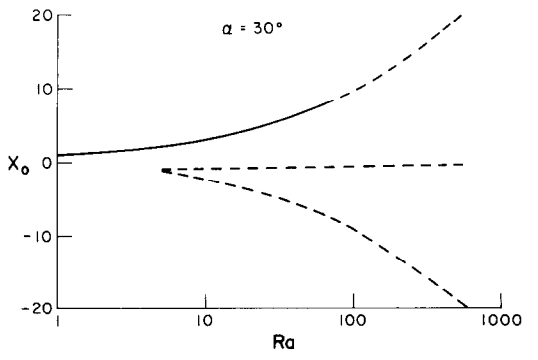

FIG. 6. Same as Fig. 5, except $\alpha = 30°$.

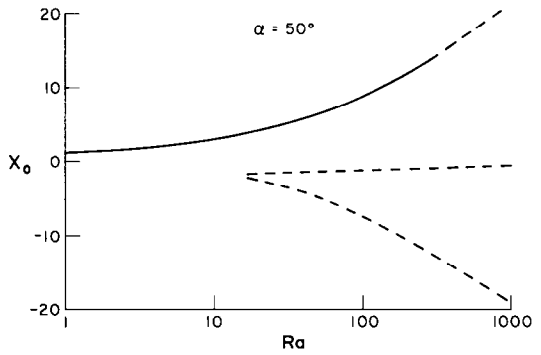

FIG. 7. Same as Fig. 6, except $\alpha = 50°$.

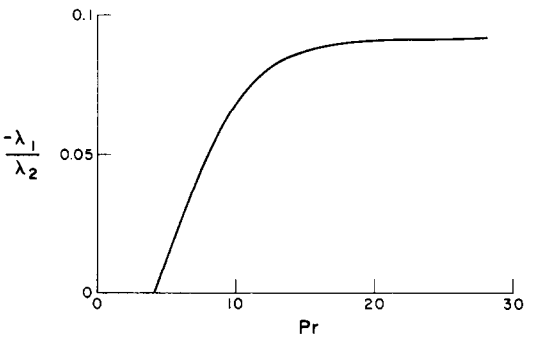

FIG. 8. Ratio of the Landau constants vs *Pr*.

4. STRONGLY NON-LINEAR MOTIONS

Because the master problem is so simple, it is possible to make some progress both analytically and numerically on the question of what happens in situations which are supercritical, where *Ra* is above the region where stable steady solutions exist. Of first importance is the evolution of the oscillatory disturbances that linear theory predicted would grow on top of the steady flow for certain values of *Ra*, *Pr* and α. A particularly interesting study in this regard was carried out for the Lorenz equations ($\alpha = 0$, $N = 1$) by McLaughlin and Martin [12]. They performed a weakly non-linear expansion about the critical values of *Ra* and *Pr* with the aim of determining the amplitude $A(t')$ of the oscillatory disturbances of linear theory. Here t' is the slow-time of a multiple time-scale expansion. They arrived at a Landau equation for A of the form

$$\frac{dA^2}{dt'} = \lambda_1 \Delta c A^2 - \lambda_2 A^4, \tag{22}$$

where the λ's are the Landau constants, and Δc is the supercriticallity

$$\Delta c = \sqrt{(Ra-1)} - \sqrt{(Ra_c - 1)}, \tag{23}$$

measuring the excess of *Ra* into the linearly unstable region delimited by the neutral parameter $Ra_c(Pr)$. Since λ_1 is positive, if Δc is positive, modes small enough in amplitude that the A^4 term can be neglected will grow exponentially by equation (22). With the quartic term taken into account the oscillatory instability will saturate to a finite value (and thus be observable at large times) if λ_2 is positive. If, however, λ_2 is negative then supercritical finite-amplitude oscillations are unstable. Although subcritical limit cycles can exist as steady solutions of equation (22) with $\Delta c < 0$, they are unstable as well. Thus $\lambda_2 < 0$ implies that no stable finite-amplitude oscillations in the vicinity of the linear neutral curve exist.

Using the formulae of McLaughlin and Martin [12] the ratio of λ_1/λ_2 was computed for various *Pr* (still with $N = 1$, $\alpha = 0$). The result is shown in Fig. 8. For all *Pr* for which the steady flow is unstable the ratio is negative. Thus there are no stable limit cycles in the vicinity of the critical points. For conditions very near critical, the time evolution may be very slow and almost-steady oscillations may appear (Fig. 9 shows one numerical example), but in an asymptotic sense one does not expect to see a constant amplitude limit cycle (since they are unstable). Oscillations have, however, been reported by Greif *et al.* [6] in their numerical finite-difference solutions of the partial differential equation model, but a close look at what they call 'periodic' reveals in fact a slowly decaying oscillation. For conditions near critical, it is obviously necessary to carry out very long runs, and this is where the reduction to three ODEs becomes very valuable.

In the slightly subcritical case it is now well known that certain initial conditions close to the steady flow evolve into the steady flow, but initial conditions far away spiral out into a chaotic solution. Chaos is possible since trajectories not captured by a fixed-point in the phase space of equations (11)–(13) must be bounded, must collapse onto a surface of dimension less than 3 (this is easily shown following the method originally used by Lorenz [9]), and cannot fall onto a stable limit cycle for values of $Ra \approx Ra_c$ since there aren't any. The orbit must then be aperiodic. Note that Fig. 9 shows an oscillation decaying slowly to a steady value, where the initial condition is close to that value. Figure 10 shows the result of a numerical integration of equations (11)–(13) using a Runge–Kutta scheme with a step size of 0.005 and starting with an initial condition far from the stable steady root. It is convenient to categorize the solutions in terms of their orbits in the XY plane. The trajectory falls onto a strange or chaotic attractor, with aperiodic oscillations about the two stable fixed-points (note that the value of *Ra* used is below the critical value). The trajectories are 'protected' from the stable and locally attracting fixed-points by the surrounding unstable limit cycle. Numerous integrations for other values of N indicate that in general one does not find any stable limit cycles near the critical values of *Ra* where the linear theory predicts a growing oscillation, rather one finds only chaotic motions for *Ra* in excess of critical, and steady or chaotic motions for subcritical *Ra*, depending on the initial conditions.

It has been shown that the Lorenz system does have

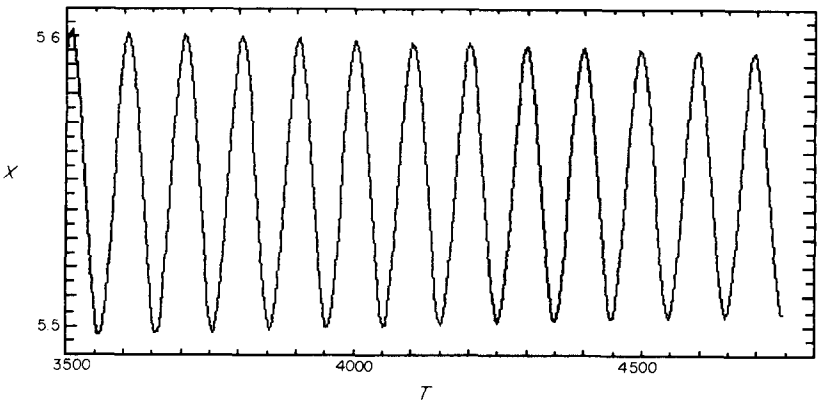

FIG. 9. Time trace after 3500 time steps: $Ra = 68$, $N = 0.55$, $Pr = 2.24$, $\alpha = 0$, $X(0) = 5.4$.

stable periodic solutions for very large Ra (Manneville and Pomeau [13], Shimizu and Morioka [14], Robbins [15]) and they have been found numerically here for general N and α as well. However, the required values of Ra are well beyond those used in any existing or probable experimental studies (for example, in ref. [14] periodic solutions are found to re-appear at $Ra = 340$–1000, or at least 20 times the critical Ra for linear instability). There are also small islands of periodic behavior embedded in a sea of chaos for large Ra as well [13, 14]. These are beyond the scope of this paper, and are probably not important for realistic thermosyphons because the required value of Ra is so large. Figure 11 shows typical solution trajectories for small but non-zero α. The flow evolves to one of the two steady roots if the initial conditions are within its domain of attraction. No attempt has been made here to find out precisely what the domains are, but it is likely that the fact that Damerell and Schoenhals [8] did not

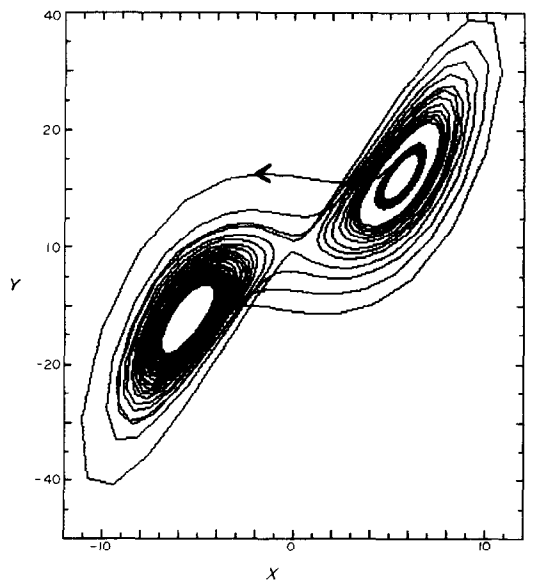

FIG. 10. Phase projection for $Ra = 68$, $N = 0.55$, $Pr = 2.24$, $\alpha = 0$, $X(0) = 0.1$.

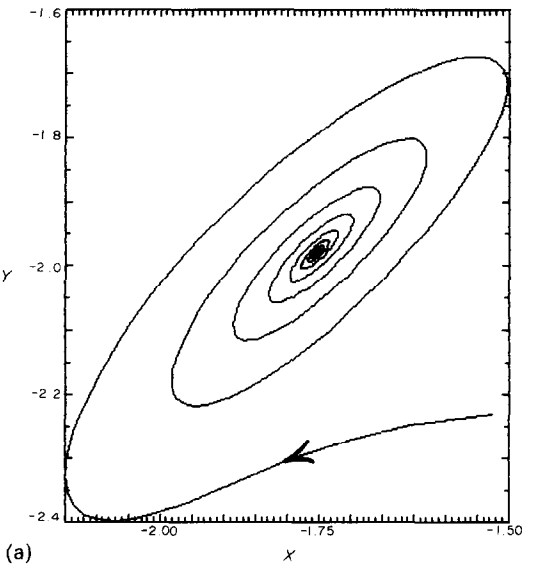

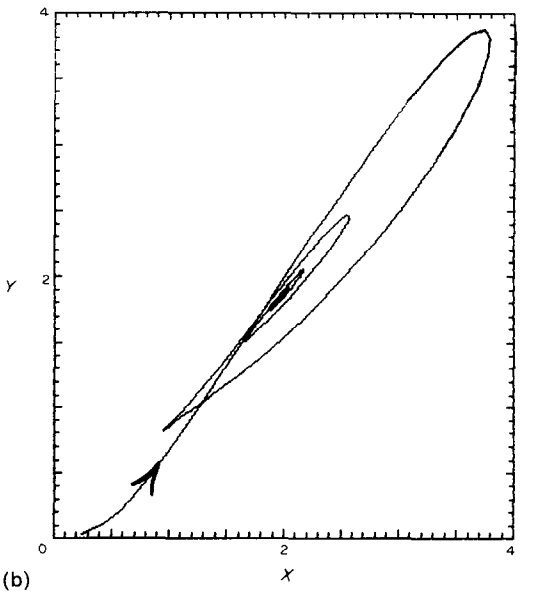

FIG. 11. Phase projection for $Ra = 4.6$, $N = 1.0$, $Pr = 7.0$, $\alpha = 10°$. (a) $X(0) = -1.3$; (b) $X(0) = 0.001$.

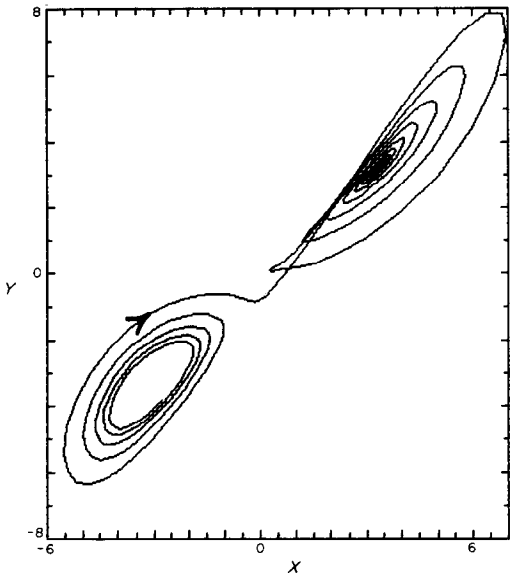

FIG. 12. Phase projection for $Ra = 11.4$, $N = 1.0$, $Pr = 7.0$, $\alpha = 10°$, $X(0) = -3.10$.

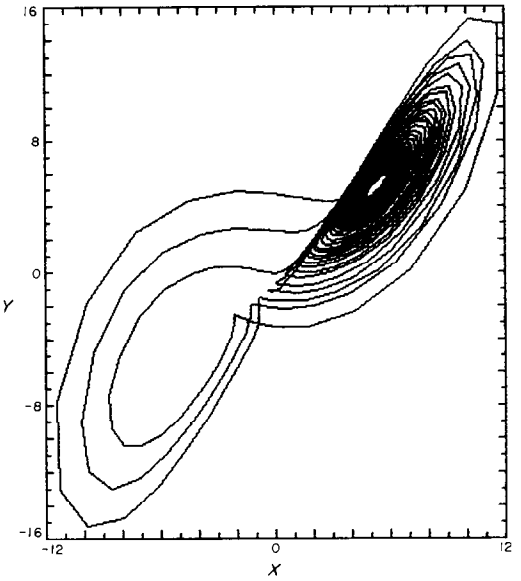

FIG. 13. Phase projection for $Ra = 28.4$, $N = 1.0$, $Pr = 7.0$, $\alpha = 10°$, $X(0) = -4.00$.

find any counter-rotating steady flows at small angles was a result of their not having a counter-rotating initial condition.

Figure 12 shows that if the negative root at $\alpha = 10°$ is unstable, and an integration is started near it, the solution will spiral away from this root onto the positive steady root if it is stable, otherwise the system will become chaotic as shown in Fig. 13. Of course if the positive steady root is only slightly unstable, the negative one will be very unstable and in the chaotic regime the system will spend a greater majority of its time oscillating aperiodically in the vicinity of the positive co-rotating root. This typical behavior is reflected in the time trace for this integration (Fig. 14).

Lastly it is shown that the tendency of decreasing N to stabilize the steady flows carries over into the non-linear regime. Figure 15 shows two sections for (a) $N = 1.0$ and (b) $N = 0.55$ and a large value of Ra. Note that at $N = 1$ the system evolves onto a strange attractor with chaotic orbits, while at $N = 0.55$ the initial state spirals into a steady fixed point.

5. CONCLUSIONS

It has been shown that the 1-D thermosyphon model, that is usually given as two coupled first-order non-linear partial differential equations, can be reduced exactly to three coupled non-linear ordinary differential equations. A stability analysis for steady solutions of these equations has been carried out along with several numerical integrations. The primary goal of this study was to obtain a simple characterization of the state of motion after the decay of initial transients in the thermosyphon.

The stability and numerical results indicate a substantial sensitivity to the frictional drag law used. The intervals of parameter space where one expects to find stable steady motions are enlarged when a

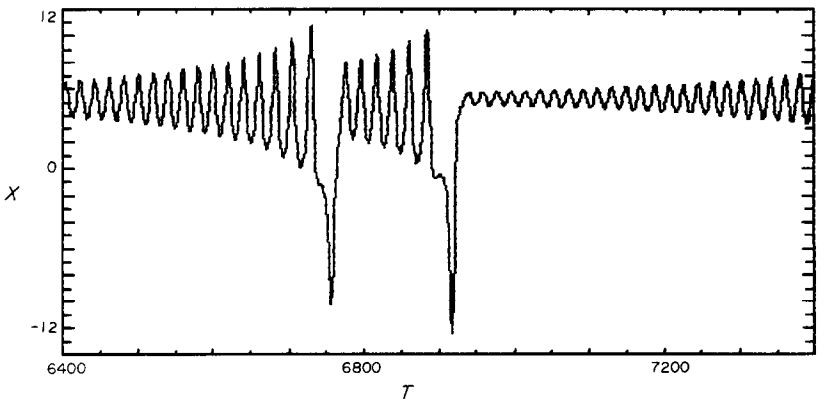

FIG. 14. Time trace after 6400 steps for conditions as in Fig. 13.

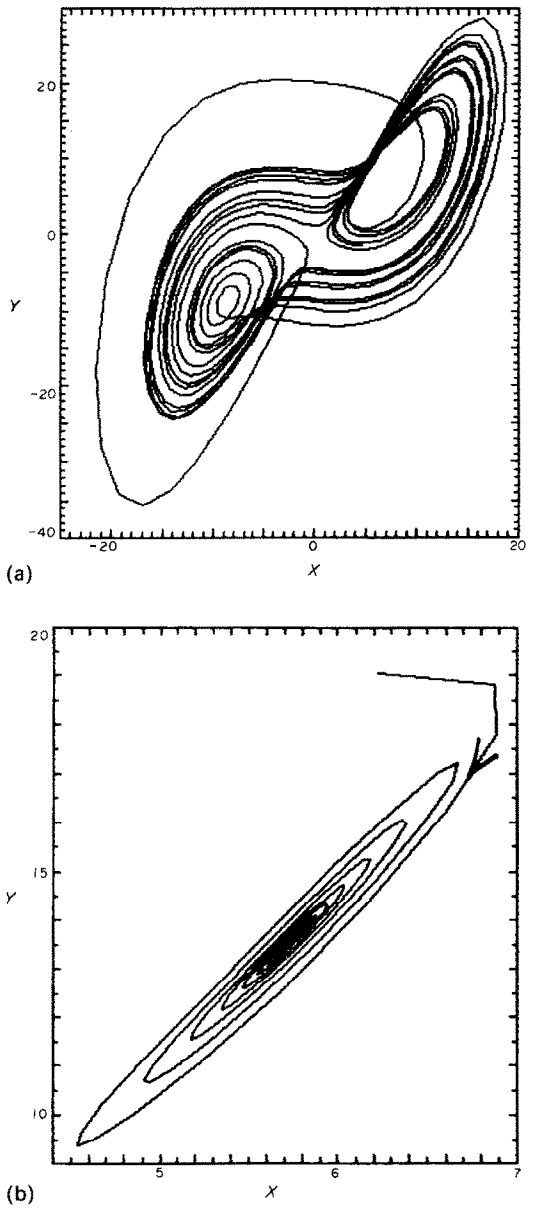

FIG. 15. Phase projection for $Ra = 80$, $Pr = 7.0$, $\alpha = 5.0$, $X(0) = 4.0$. (a) $N = 1.0$; (b) $N = 0.5$.

turbulent drag law is used. For sideways heating at an angle α, multiple stable steady states are possible for small α. As Ra is raised, the counter-rotating steady solution becomes unstable before the co-rotating one. At a large angle and small N, the co-rotating steady flow is found to be stable at very large Ra.

When there are multiple steady states the system evolves to the one that is 'closest' to the initial state in phase space. When there is one stable fixed-point surrounded by an unstable limit cycle (the inverted Hopf bifurcation), the system evolves either to a steady state or to a chaotic state depending on the initial conditions. If there are no stable fixed-points the system can become chaotic for values of Ra that are not so large as to be unrealistic. Thus although linear theory predicts an oscillatory instability with two complex conjugate eigenvalues crossing the imaginary axis (the Hopf bifurcation), in no case could a stable limit cycle be found for Ra less than several hundred. This suggests that experimentally observed oscillations may really have been just slowly decaying or slowly growing, not steady.

Previous experimental observations [5, 8] have shown that as Ra is increased through the chaotic flow regime, a bifurcation back to steady flow is observed. Since the present model does not show any stable steady solutions for large Ra, this study agrees with the suggestion given in ref. [5] that the return to steady flow in the experiments is caused by an internal change in the drag law.

Most of the papers cited in the introduction that look at the closed toroidal thermosyphon do not systematically deal with stability, instead concentrating on steady flows and/or relatively few and short numerical integrations of equations (1) and (2) using comparatively complicated finite-difference schemes. It has been shown that both the linear stability and the non-linear transient behavior can be examined very simply but that long integrations are needed to reach statistical equilibrium. One direct point of connection with the present analysis is the stability experiment of ref. [5]. Using the facts that the θ-average of $T^* = 0$ and that $Q = 2q_s/R_p$, along with data from their Fig. 9, Table 1, and equations (4) and (7), one finds that their experiment becomes chaotic (they use the word 'unstable') at $Pr = 4.83$, $N = 1.17$, and $Ra = 11.7$. The present theory gives a critical value of $Ra = 9.09$ at the same values of Pr and N. The difference is remarkably small given the approximations used to derive equations (1) and (2).

Here only the friction parameterization has been discussed. It is not obvious that the heat transfer coefficient h should only be a function of position. If v gets large enough, h should reflect a transition to forced convection [that is, h should become $h(v)$]. As long as h is only a function of v and θ, not T, the mathematical reduction scheme will work. One still gets a system of three ordinary differential equations although the non-linear coupling will be more complicated.

Acknowledgement—This research was supported by a grant ATM-8111718 from the National Science Foundation.

REFERENCES

1. P. Welander, On the oscillatory instability of a differentially heated fluid loop, *J. Fluid Mech.* **29**, 17–30 (1967).
2. K. E. Torrance, Open-loop thermosyphons with geological applications, *J. Heat Transfer* **101**, 677–683 (1979).
3. H. H. Bau and K. E. Torrance, Transient and steady behavior of an open, symmetrically heated, free convection loop, *Int. J. Heat Mass Transfer* **24**, 597–609 (1981).
4. A. Mertol, R. Greif and Y. Zvirin, Two dimensional study of heat transfer and fluid flow in a natural convection loop, *J. Heat Transfer* **104**, 508–514 (1982).

5. H. F. Creveling, J. F. De Paz, J. Y. Baladir and R. J. Schoenhals, Stability characteristics of a single-phase free convection loop, *J. Fluid Mech.* **67,** 65–84 (1975).
6. R. Greif, Y. Zvirin and A. Mertol, The transient and stability behavior of a natural convection loop, *J. Heat Transfer* **101,** 684–688 (1979).
7. A. Mertol, R. Greif and Y. Zvirin, The transient, steady state and stability behavior of a thermosyphon with throughflow, *Int. J. Heat Mass Transfer* **24,** 621–633 (1981).
8. P. S. Damerell and R. J. Schoenhals, Flow in a toroidal thermosyphon with angular displacement of heated and cooled sections, *J. Heat Transfer* **101,** 672–676 (1979).
9. E. N. Lorenz, Deterministic nonperiodic flow. *J. Atmos. Sci.* **20,** 130–141 (1963).
10. E. Ott, Strange attractors and chaotic motions of dynamical systems. *Rev. Mod. Phys.* **53,** 655–671 (1981).
11. O. E. Lanford, III, The strange attractor theory of turbulence, *Ann. Rev. Fluid Mech.* **14,** 347–364 (1982).
12. J. B. McLaughlin and P. C. Martin, Transition to turbulence in a statically stressed fluid system, *Phys. Rev.* **A12,** 186–203 (1975).
13. P. Manneville and Y. Pomeau, Different ways to turbulence in dissipative dynamical systems. *Physica* **D1,** 219–226 (1980).
14. T. Shimizu and N. Morioka, Chaos and limit cycles in the Lorenz model, *Phys. Lett.* **66A,** 182–184 (1978).
15. K. A. Robbins, Periodic solutions and bifurcation structure at high R in the Lorenz model, *SIAM J. Appl. Math.* **36,** 457–472 (1979).

APPENDIX

Here some simple results for the slaved modes are discussed. One drops the index n and sets $H_n/H_1 = -1$, since all the problems are similar in structure. The equations become

$$\frac{dC}{dt} = -C - XS, \tag{A1}$$

and

$$\frac{dS}{dt} = -S + XC - Ra. \tag{A2}$$

Assume a solution exists. Let $C = C_0 + c, S = S_0 + s$, where C_0 and S_0 are the known solutions and c and s are finite-amplitude perturbations. Substituting these forms into equations (A1) and (A2), subtracting the known solution, multiplying equation (A1) by c and equation (A2) by s, and adding, yields

$$\frac{d(s^2+c^2)/2}{dt} = -(s^2+c^2). \tag{A3}$$

Thus if a solution exists it will be stable. All finite perturbations decay exponentially.

Assume there are two solutions. Let these be C_1, C_2 along with S_1, S_2 where the subscript is not to be confused with the Fourier index used in equations (14) and (15). Form A1(1) $\times C_1$, A1(2) $\times C_2$, A1(1) $\times C_2$, and A1(2) $\times C_1$ along with similar equations for the S's. Here A1(1) denotes equation (A1) using C_1 and S_1, and so on. The resulting eight equations can be combined into

$$\frac{d[(S_1-S_2)^2+(C_1-C_2)^2]}{dt} = -2[(S_1-S_2)^2+(C_1-C_2)^2]. \tag{A4}$$

Thus at large time the phase space distance between these solutions must exponentially decrease to zero showing that there is only one unique and stable solution.

When X becomes steady at large time, the complete temperature field is given uniquely by the steady solution of equations (14) and (15). This is, returning to the Fourier index

$$C_n = -nXS_n, \tag{A5}$$

and

$$S_n = Ra\, H_n H_1 (1+n^2X^2), \tag{A6}$$

which will converge if H_n decreases with n.

If X evolves to a periodic solution of period m, equations (14) and (15) can be solved by assuming a solution of the form

$$C_n = \sum_{k=0\to\infty} C_{nk} \exp(i\, mkt). \tag{A7}$$

An infinite matrix is obtained for the coefficients. The truncated determinant can be shown to be not zero, so a solution will exist. However, since no periodic solutions for reasonable Ra have been found this point was not pursued.

If X is chaotic, then the linear equations have random coefficients, and the solutions will contain chaotic components as well.

UNE NOUVELLE ANALYSE DU THERMOSYPHON EN BOUCLE FERMEE

Résumé—Cette étude théorique concerne la nature des mouvements dans une boucle torique orientée dans un plan vertical et soumise à un chauffage interne plutôt général et/ou à des conditions thermiques à la paroi. On montre que les modèles d'écoulement monodimensionnel peuvent être transformés, sans autre approximation, en un problème-clé à trois équations différentielles non linéaires. Le flux massique est déterminé par le problème-clé. La question d'existence et de stabilité des écoulements permanents conduit à des équations algébriques cubiques. Dans le régime fortement non-linéaire, on montre que les écoulements permanents ou chaotiques non périodiques, sont seuls possibles. On décrit la sensibilité des prévisions du modèle monodimensionnel aux différentes paramétrisations du frottement pariétal.

EINE NEUE UNTERSUCHUNG DES 'CLOSED-LOOP'-THERMOSYPHONS

Zusammenfassung—Diese theoretische Untersuchung befaßt sich mit den Bewegungsabläufen in einem torusförmigen Fluid-Kreislauf, der in einer senkrechten Ebene orientiert ist und den unterschiedlichsten inneren thermischen Wandbedingungen ausgesetzt wird. Es wird gezeigt, daß sich frühere eindimensionale Modelle der Kreislauf-Strömung ohne weitere Approximationen transformieren lassen, und zwar in ein 'master'-Problem, das aus drei nichtlinearen gewöhnlichen Differentialgleichungen besteht, und einen unendlich großen Satz von linearen 'slave'-Problemen. Der Massenstrom wird allein durch das 'master'-Problem bestimmt. Die Frage nach Existenz und Stabilität von stationären Strömungen wird auf die Untersuchung von kubischen algebraischen Gleichungen reduziert. Es wird ausgeführt, daß im extrem nichtlinearen Bereich nur stationäre oder chaotische Strömungen möglich sind, nicht jedoch periodisch schwankende. Die Empfindlichkeit der Voraussagen des eindimensionalen Modells im Hinblick auf verschiedene Wandschubspannungen wird beschrieben.

НОВЫЙ ПОДХОД К АНАЛИЗУ ТЕРМОСИФОНА С ЗАМКНУТЫМ КОНТУРОМ

Аннотация—Проведено теоретическое исследование характера течений в тороидальном заполненном жидкостью контуре, ориентированном в вертикальной плоскости, при довольно общих условиях внутреннего нагрева и/или тепловых условиях на стенке. Показано, что применявшиеся ранее одномерные модели для течения в контуре можно, не прибегая к дальнейшим приближениям, свести к «основной» задаче из трех нелинейных обыкновенных дифференциальных уравнений и к бесконечному множеству линейных «вспомогательных» задач. Поток массы определяется только из основной задачи. Вопрос о существовании и устойчивости стационарных течений сводится к анализу кубических алгебраических уравнений. Доказывается, что при сильно нелинейном режиме возможны только стационарные или хаотические, но не периодические течения. Показано параметрическое влияние напряжений на стенке на результаты расчетов с помощью одномерной модели.